Металлофиз. новейшие технол. / Metallofiz. Noveishie Tekhnol.
2017, т. 39, № 5, сс. 665–675 / DOI: 10.15407/mfint.40.05.0665
Оттиски доступны непосредственно от издателя
Фотокопирование разрешено только
в соответствии с лицензией

МЕТАЛЛИЧЕСКИЕ ПОВЕРХНОСТИ И ПЛЁНКИ

PACS numbers: 62.20.Qp, 68.35.Ct, 68.35.Dv, 81.15.Cd, 81.40.Pq, 81.65.Lp

Characterization of Mo–V–N Coatings Deposited on XC100 Substrate by Sputtering Cathodic Magnetron

Brahim Chermime[*,**], Abdelaziz Abboudi[*], Hamid Djebaili[**], and Mourad Brioua[*]

[*] *Department of Mechanics, Colonel Hadj Lakhdar University of Batna, 05000 Batna, Algeria*
[**] *Department of Mechanics, Abbas Laghrour University of Khenchela, 40004 Khenchela, Algeria*

The aim of this work is the characterization of ternary molybdenum–vanadium nitride (Mo–V–N) coatings deposited on silicon and XC100 steel substrates by the reactive radiofrequency dual magnetron sputtering with different contents of the Mo and V targets and nitrogen as reactive gas. The metal-target bias voltages are varied from 300 to 900 V. The hardness, surface morphology, microstructure and composition are studied by nanoindentation, scanning electron microscopy, atomic-force microscopy, and x-ray diffractometry. The Mo–V–N films manifest pyramidal surface morphology, high roughness (of 13.5 nm), but low mechanical properties. Hardness and Young's modulus are found in the ranges of 10–18 GPa and 100–335 GPa, respectively. The residual stresses of coatings are compressive and varied between 0.8 GPa and 2.5 GPa (calculated with the Stoney formula).

Keywords: coatings, microstructure, residual stresses, roughness, hardness.

Метою даної роботи є характеризація покриттів із трикомпонентного молібден-ванадійового нітриду (Mo–V–N), що наносилися на кремнійові та сталеві (XC100) поверхні шляхом реактивного радіочастотного магнетронного двокатодного розпорошення цілей із різним вмістом Mo та V із використанням азоту в якості реакційноздатного газу. Відхили напруги зміщення металевої цілі варіювалися від 300 до 900 В. Твердість, морфологію поверхні, мікроструктуру та склад було досліджено за допомогою

Corresponding author: Brahim Chermime
E-mail: cherbrah@yahoo.fr

Please cite this article as: Brahim Chermime, Abdelaziz Abboudi, Hamid Djebaili, and Mourad Brioua, Characterisation of Mo–V–N Coatings Deposited on XC100 Substrate by Sputtering Cathodic Magnetron, *Metallofiz. Noveishie Tekhnol.*, **39**, No. 5: 665–675 (2017), DOI: 10.15407/mfint.40.05.0665.

метод наноіндентування, сканувальної електронної мікроскопії, атомно-силової мікроскопії та рентґенівської дифрактометрії. Плівки Mo–V–N мають пірамідальну морфологію поверхні, високу шерсткість (13,5 нм), але низькі механічні властивості. Твердість і модуль Юнґа лежать у діяпазонах 10–18 ГПа та 100–335 ГПа відповідно. Залишкові напруження у покриттях (обчислені за формулою Стоні) є стискальними і лежать у межах між 0,8 і 2,5 ГПа.

Ключові слова: покриття, мікроструктура, залишкові напруги, шерсткість, твердість.

Целью этой работы является характеризация покрытий, изготовленных из трёхкомпонентного молибден-ванадиевого нитрида (Mo–V–N), которые наносились на кремниевые и стальные (XC100) подложки с помощью реактивного радиочастотного магнетронного двухкатодного распыления мишеней с различным содержанием Mo и V с использованием азота в качестве реагирующего газа. Напряжения смещения металлической мишени варьировались от 300 до 900 В. Твёрдость, морфология поверхности, микроструктура и состав изучались при помощи наноиндентирования, сканирующей электронной микроскопии, атомно-силовой микроскопии и рентгеновской дифрактометрии. Плёнки Mo–V–N обладают пирамидальной морфологией поверхности, высокой шероховатостью (13,5 нм), но низкими механическими свойствами. Твёрдость и модуль Юнга находятся в диапазонах 10–18 ГПа и 100–335 ГПа соответственно. Остаточные напряжения в покрытиях (рассчитанные по формуле Стони) являются сжимающими и изменяются в пределах от 0,8 до 2,5 ГПа.

Ключевые слова: покрытия, микроструктура, остаточные напряжения, шероховатость, твёрдость.

(Received March 22, 2017; in final version, April 10, 2017)

1. INTRODUCTION

Molybdenum nitride is a transition metal nitride and interstitial compound. As many other transition metal nitrides, molybdenum nitride has good physical and chemical properties, including high hardness, good electrical conductivity, wear and corrosion resistance. Molybdenum nitride also has unique electronic, magnetic, superconducting and catalytic properties that are similar to noble metals in many aspects. Because of these excellent properties, molybdenum nitride has found wide application in modern industry such as wear and corrosion resistant coatings and catalyst. The existence of the Mo–N phase in stainless steel was reported to enhance the hardness of the bulk material [1]. The thin surface layer affects the properties of tools, particularly their service life, durability and performance and thus increases work productivity and decreases costs of machining [2]. The following three basic types of standard layers have been used most frequently in

commercial applications: Ti–N, Ti–Al–N, Ti–C–N and their multilayer and gradient modifications [3].

The superconducting properties of Mo–N thin film also have been investigated [4, 5]. Mo–N films can be prepared with various type processes. A sputtered Mo film implanted with nitrogen will produce γ-Mo_2N, *B*1-Mo–N, and δ-Mo–N and lead to changes in the optical properties [6]. In this article, we filed ternary Mo–V–N coatings on carbon steel substrates XC100 and silicon using a magnetron Physical Vapour Deposition sputtering system with the Mo and V objectives and nitrogen as gas reactive. The nitride molybdenum vanadium (Mo–V–N), a ternary nitride by incorporation of V and Mo, the Mo–V–N coatings have been reported having good oxidation resistance without compositional and structural changes after both as molybdenum and vanadium can form protective oxides which have eliminated the diffusion of oxygen into the substrate.

Molybdenum nitride is an attractive candidate for the diffusion barrier owing to its high conductivity and resistance of diffusion to foreign atoms. During the past two decades, several works [7–11] have been reported regarding molybdenum nitride as diffusion barriers. In magnetron sputtering, a magnetic field is applied to avoid the loss of electrons in the plasma, by placing a magnet (magnetron) behind the target. The magnetic field generated, traps the electrons in the plasma, in a region between the target and the substrate, and helps producing more ions. This allows us to work at low gas pressures and with relatively low target voltages [12]. If a reactive gas (nitrogen here) is instead introduced into the chamber, it reacts with the sputtered material to form a compound on the substrate. This technique is called reactive magnetron sputtering [13].

2. EXPERIMENTAL PROCEDURE

Mo–V–N thin films were deposited by radiofrequency (RF) dual magnetron sputtering (NORDIKO type 3500–13.56 MHz, 1250 W) in an Ar/N_2 mixed atmosphere on Si (100) coupons (10×10 mm^2, 380 μm thick) and polished XC100 steel discs ($d = 15$ mm, 3 mm thick) with the Mo and V targets and argon, nitrogen as reactive gas. The sputtering rate obtained for 600 eV the energy of Ar ions 0.92 for Mo and 1.2 for V. The following chemical composition (% wt.) (see Table 1).

In this study, Mo (99.95 at.%) and V (99.96 at.%) targets were used

TABLE 1. Chemical composition of XC100 steel.

XC100	C	Mn	Si	Cr	Ni
% wt.	0.95–1.1	0.25–0.4	0.1–0.35	1.3–1.6	0.3

to co-deposit the Mo–V–N films. The Mo and V targets were cleaned with an Ar + discharge for 8 min at 250 W (500 V) to obtain 230–250 nm thick Mo (or V) underlayers to improve adhesion, the distance between the confocal arranged targets and the substrate was 70 mm. Table 2 gives conditions of Mo–V–N coating deposition. In the second part of this study, Mo–N and Mo–V–N films were deposited using DC/RF dual magnetron sputtering system (AC450). ADC and RF (13.56 MHz) generator were used to polarize the Mo and V targets. The substrates were fixed on a vertical support which is polarized in DC (1000 V) and the potential float .The structure of the coatings was analysed by XRD.

The average grain size of the thin films was determined by Scherrer's method [14]:

$$D = \frac{0.9\lambda}{\beta \cos\theta}, \tag{1}$$

where 0.9 is the shape factor, λ represents the X-ray wavelength, which used for the measurement ($\lambda_{Co} = 0.178$ nm), the line β is the line width (FWHM) in radians, θ is the Bragg's angle.

The position of the (111) diffraction peak was used to estimate the grain size. The measurement of apparent microhardness (obtained in 1 mN of lading) and the Young's modulus of these coatings is carried out using a nanoindentation (XP–MTS) (typical pyramidal Berkovitch indenture) according to the method developed by [15]. The compressive residual (σ) of these coatings stresses are calculated with the Stoney formula [16]:

$$\sigma = \pm \frac{E_S}{6(1-\nu_s)} \frac{e_s^2}{e_f} \left(\frac{1}{R} - \frac{1}{R_0} \right). \tag{2}$$

Here, σ is the residual stress in the thin film, E_s and ν_s are Young's modulus (195 GPa) and Poisson's ratio (0.29) of the substrate, e_f and e_s

TABLE 2. Deposition conditions of the Mo–V–N coating.

Coating	Targets bias, [V]		Nitrogen in the plasma, %	Deposition time, min
	V	Mo		
Mo–V–N	300	900	20	80
	500			
	700	700		
	900	500		
		300		

indicate the film and substrate thicknesses, respectively, R is the curvature radius of the sample after deposition, R_0 the curvature radius before deposition.

The pin-on-disc and oscillating (TRIBO tester) wear tests were carried out to characterize the tribological performance of the coatings. The counterparts were $100Cr_6$ steel balls, 6 mm in diameter. The applied load was increased progressively from 0 to 5 N within the sliding speed was 0.5 m/s. The maximum sliding distance was 600 mm and the wear track diameter was 2 mm under a test temperature of 21.5°C and a relative humidity of 33.2%. Each test lasted about 10 min. During the measurement, the experimental parameters such as transverse force and acoustic emission are recorded for the subsequent data analysis.

3. RESULTS AND DISCUSSION

According to the spectrum of X-rays diffraction in Fig. 1, we note that in addition to the peaks (110), (211) and (200) of the cubic structure α-Fe, there are also peaks (111) of the tetragonal structure Mo_2N, which is present for all concentrations of nitrogen. For the low nitrogen con-

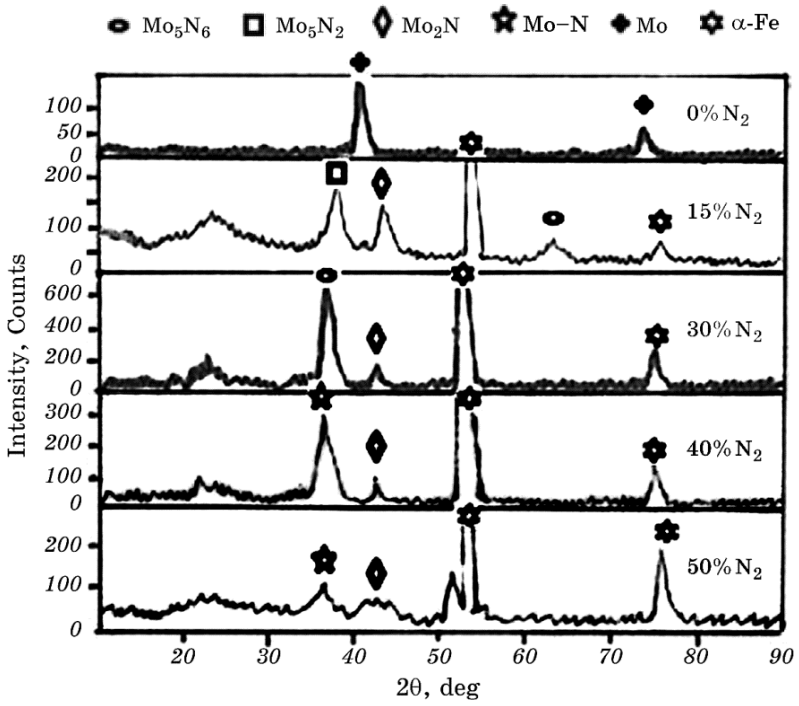

Fig. 1. Spectra of the thin Mo and Mo–N films.

centrations (< 10% N_2) in the sputtering gas, cubic Mo_3N_2 is formed and transforms to hexagonal structure Mo_5N_6 (for 30% N_2). Increasing the N_2 concentration to 40% N_2 results in a strong hexagonal Mo–N peak. Mo_2N and Mo–N phases are identified as β-Mo_2N and δ-Mo–N [17].

However, the intensity of the Mo–N peak reduces drastically [18], with increase in N_2 concentration from 40% to 50% amorphous phase or phase, which tends to become nanocrystalline [19], have determined that the nitrogen and molybdenum sites are fully occupied for the highly-ordered δ-Mo–N phase with lattice parameters of $a = 0.573659$ nm and $c = 0.561884$ nm [19]. The XRD peaks corresponding to the δ-Mo–N phase observed in Fig. 1 have lattice constants of $a = 0.574$ nm and $c = 0.5622$ nm, which are very close to those reported by [19]. Which suggest the formation of a highly ordered δ-Mo–N phase. Furthermore, the peak intensity decreases as the Mo_2N nitrogen concentration increases. It should be not end here that all the peaks of Mo–N are not properly aligned with PDF files (*i.e.*, the positions of these peaks are translated to smaller 2θ angles), so large interplanar distances. This one can only be explained by a deviation from stoichiometry of the layer, the N/Mo ratio being greater than 1, and therefore the insertion probable nitrogen atoms in interstitial sites.

The analysis of the XRD patterns (Mo–N, Mo–V–N and V–N) was presented in Fig. 2. We note that most of the peaks of phases: Mo_2N (111), Mo_2N (200) and α–Fe, there are also V–N peaks (111) and V–N (200) respectively in 43.96°C and 51.83°C, and the peaks of low inten-

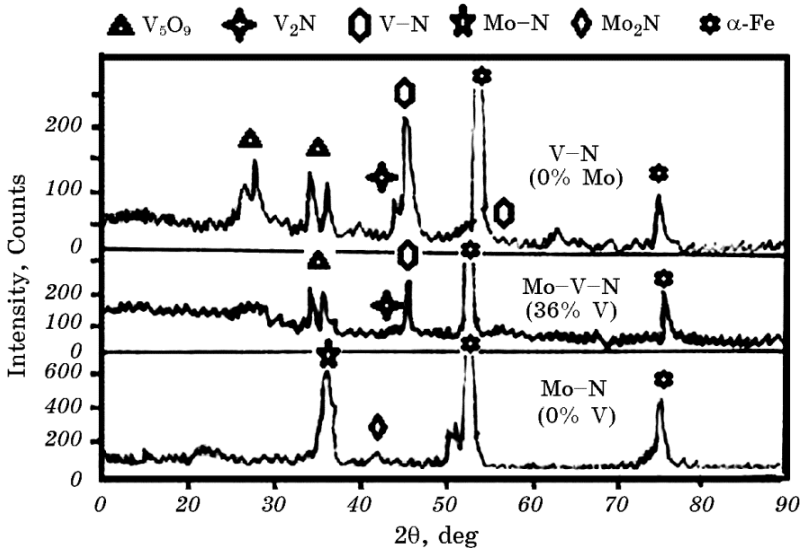

Fig. 2. Spectra of the Mo–N, Mo–V–N, and V–N coatings.

sity of V_2N (110) at 43.03°C. These peaks were also detected for the coatings (V–Ti–N) [20]. A vanadium oxide V_5O_9 (101) and (0–22) of low intensity peaks were also detected respectively at 30.58°C and 35.50°C. In contrast, the V–N (111) and V_2N (110) orientations gradually emerge that is probably caused by the increase in the applied power of the V target (bias voltage). This suggests that the Mo–V–N films are a solid solution composed of Mo and V, where Mo atoms are substituted by V ones.

Moreover, as the structural property and the lattice constants of Mo–N and V–N are very similar, this is not so easy to determine the real composition of these Mo–V–N phases. V–N is of interest for the applications requiring hard and corrosion resistant materials [21]. In the Mo–V–N coatings, as a function of the Mo and V targets, we observe no presence of C in our coatings, and they present up to 4 at.% of oxygen, which is negligible for the mechanical applications. The V content in increases between 0 and 29 at.% with the Mo target bias. This result can be explained by the resulting increase of the V-target sputtering rate. However, between 700 and 900 V, we note a weak increase of the V content from 28 to 31 at.% for the same target bias, molybdenum has a higher sputtering rate than vanadium it was logical that fixing the Mo target bias and, varying V, one would to obtain a maximum of V in the (V,Mo)N films as 45 at.%. It is noteworthy that V content increases with the V target bias, and the maximum value was about 31 at.% obtained at 900 V in Fig. 3.

We see the variation of the hardness and Young's modulus of the Mo–N and Mo–V–N coatings for both the Mo and V targets that is

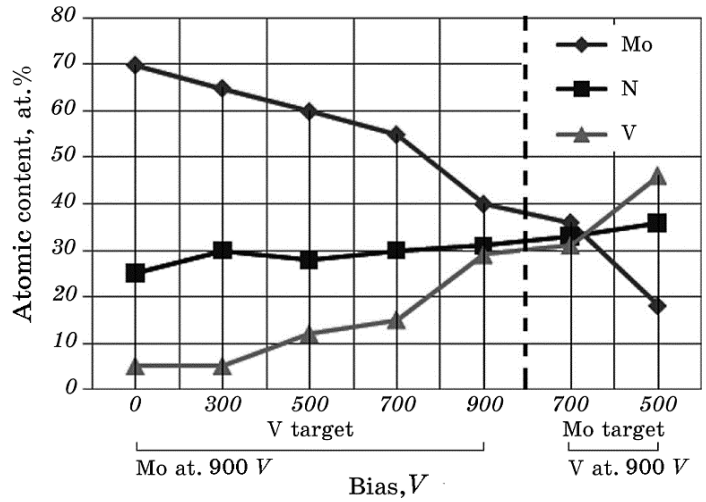

Fig. 3. Composition of the different elements as a function of the voltage applied to the V and Mo targets.

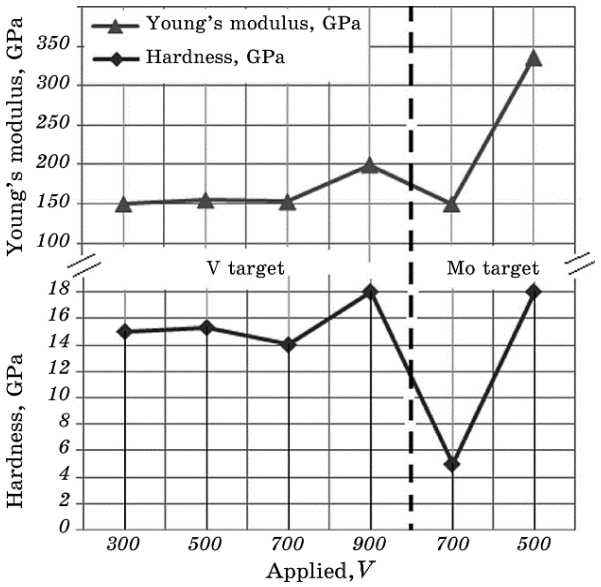

Fig. 4. Hardness, Young's modulus of thin Mo–V–N films as a function of V.

shown in Fig. 4.

The relaxation of residual stress directly affects the hardness of (Mo,V)N coatings. We note the slight decrease in residual stresses when the voltage increases for both the Mo and V targets. We see that the compressive residual stresses have the same trend as the hardness and the Young's modulus, residual stresses vary between 0.8 and

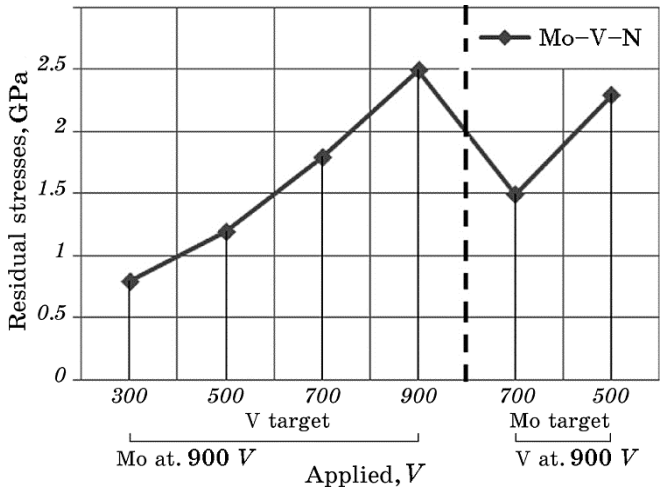

Fig. 5. Residual stresses depending on the applied voltage.

2.5 GPa the layer (to 900 V) (see Fig. 5).

Two phenomena could explain the variation of the residual stress; the substitution of the atoms of V by Mo and the energy of the sort (species) or the incidental atoms during the process of cathodic spraying (pulverizing), the residual stress increase with the contents of vanadium until their the highest value for 28% of V, then they decreased. These maximal values correspond to the training (formation) of the systems $Mo_{0.4}V_{0.28}N_{0.3}$ which are more put under stress than Mo–N because of the setting-up (presence) of V atoms in Mo–N.

The morphology and the atomic-force microscope (AFM) is used to produce images of our films in order to determine their microstructures, to measure the roughness of the surface studied until a resolution near the atomic scale (in our case, the roughness of 73.2 nm pass to 5 nm for the Mo–N coating and of 13.5 nm to 1 nm for the Mo–V–N coating), and to determine the grain size or to characterize the porosity of a layer. The choice of the applied force and the distance between the tip and the surface of the film was made to bring enough a hard tip in order to realize the scan, while avoiding the deformation of the tip or the sample surface. Figure 6 shows the AFM images of a surface of 9 μm^2 films Mo–N and Mo–V–N obtained on substrates of silicon Mo–N (Fig. 6, *b*).

We observe that all the films exhibit a fibrous and homogeneous structure, a low porosity. The modules of the Mo–V–N film sizes (Fig. 6, *a*) are larger than those for the Mo–N film. The Mo–N layer appears less dense than Mo–V–N, but Mo–N columns are larger than those of Mo–V–N.

The introduction of V into the Mo–N film contributes to the reduction of grain size in the layers of Mo–V–N seems less porous than Mo–N. The Mo–V–N coating also reveals a dense columnar structure with a small grain size and higher RMS roughness. According to the Mathieu SMZ23, this structure is compatible with zone II.

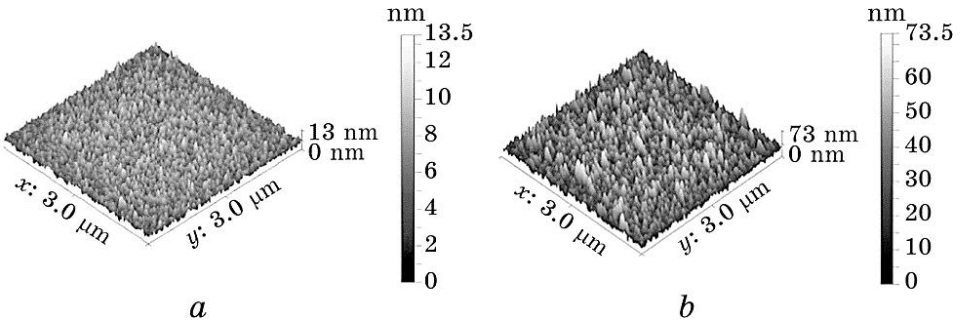

Fig. 6. AFM surface morphologies of Mo–V–N (*a*) and Mo–N deposited on Si (*b*).

4. CONCLUSIONS

Vanadium directly affects the physical-chemical and structural properties; residual stresses are studied. Of the above results, the following ones can be deduced.

1. A rough faceted grain structure with pyramid-like forms was observed for the Mo–V–N films. According to the XRD, we can suppose that the Mo–V–N coatings are composed of the solids. The Mo–N film is well crystallized; it is very dense and presents good mechanical properties solve by substitution.

2. We note the decrease in residual compressive stresses when we increased the voltage V of a target can be explained by replacing Mo atoms with V atoms.

3. The second point is the increase of residual stresses causes the energy of the incident species of atoms during the sputtering process.

ACKNOWLEDGEMENTS

We would like to thank Pr. H. Djebaili and Active Devices and Materials Laboratory, Larbi Ben M'hidi University (Oum el Bouaghi, 04000, Algeria).

REFERENCES

1. A. W. Kirby and D. J. Fray, *J. Mater. Sci. Lett.*, **12**, Iss.9: 633 (1993).
2. J. Sondor, Strojárstvo/Strojírenství, **6**: 70 (2005) (in Slovak).
3. J. Šošovičková, *Modification of Surface Properties of Metal Materials by PVD Methods* (Thesis of Disser.) (Brno: Univerzita Obrany v Brne: 2005) (in Slovak).
4. G. Linker, R. Smithey, and O. Meyer, *J. Physics F: Metal Physics*, **14**, No. 7: L115 (1984).
5. S. B. Qadri, W. W. Fuller, K. E. Kihlstrom, R. W. Simon, E. F. Skelton, D. VanVechten, and S. A. Wolf, *J. Vac. Sci. & Tech.*, **3**: 664 (1985).
6. T. Hirata and K. Saito, *J. Mater. Sci. Lett.*, **9**, Iss. 7: 827 (1990).
7. Jeong-Youb Lee and Jong-Wan Park, *Jpn. J. Appl. Phys.*, **35**, Part 1, No. 8: 4280 (1996).
8. J.-Ch. Chuang, Sh.-L. Tu, and M.-Chi. Chen, *Thin Solid Films*, **346**, Iss. 1–2: 299 (1999).
9. V. P. Anitha, S. Major, D. Chandrashekharam, and M. Bhatnagar, *Surf. Coat. Tech.*, **79**, Iss. 1–3: 50 (1996).
10. K. K. Shih and D. B. Dove, *J. Vac. Sci. Technol. A*, **8**, Iss. 3: 1359 (1990).
11. K.-L. Lin and Y.-J. Ho, *J. Vac. Sci. Technol. A*, **13**, Iss. 6: 2872 (1995).
12. J. Birch, S. Tungasmita, and V. Darakchieva, *Magnetron Sputter Epitaxy of AlN, in Nitrides as Seen by the Technology* (Eds. T. Paskova and B. Monemar) (Kerala: Research Signpost: 2002).
13. P. M. Martin, *Handbook of Deposition Technologies for Films and Coatings* (William Andrew: 2009), p. 936.

14. A. L. Patterson, *Phys. Rev.*, **56**, Iss. 10: 978 (1939).
15. L. Wang, X. Nie, J. Housden, E. Spain, J. C. Jiang, E. I. Meletis, and A. Leyland, *Surf. Coat. Technol.*, **203**, Iss. 5–7: 816 (2008).
16. G. G. Stoney, *Proc. R. Soc. A.*, **82**, Iss. 553: 172 (1909).
17. K. Inumaru, K. Baba, and S. Yamanaka, *Chem. Mater.*, **17**, Iss. 24: 5935 (2005).
18. M. Nordin, M. Larsson, and S. Hogmark, *Surf. Coat. Technol.*, **106**, Iss. 2–3: 234 (1998).
19. C. L. Bull, P. F. McMillan, E. Soignard, and K. Leinenweber, *J. Solid State Chemistry*, **177**, Iss. 4–5: 1488 (2004).
20. H. Gueddaoui, G. Schmerber, M. Abes, A. Guemmaz, and J. C. Parlebas, *Catalysis Today*, **113**, Iss. 3–4: 270 (2006).
21. U. Wiklund, B. Casas, and N. Stavlid, *Wear*, **261**, Iss. 1: 2 (2006).